Electronic structure of ladder cuprates

T. F. A. Müller, V. Anisimov, and T. M. Rice
Institut für Theoretische Physik, ETH-Hönggerberg, CH-8093 Zurich, Switzerland

I. Dasgupta and T. Saha-Dasgupta
Max-Planck-Institut für Festkörperforschung, D-70569 Stuttgart, Federal Republic of Germany

(Received 28 January 1998)

We study the electronic structure of the ladder compounds $SrCu_2O_3$ and $Sr_{14-x}Ca_xCu_{24}O_{41}$. Our local-density approximation calculations for $SrCu_2O_3$ give similar Cu $3d$ bands near the Fermi energy as reported for $Sr_{14-x}Ca_xCu_{24}O_{41}$. The hopping parameters estimated by fitting these bands show a strong anisotropy between the $t_\perp$ and $t_\parallel$ intraladder hopping and small interladder hopping. A downfolding method shows that this anisotropy arises from the ladder structure. The conductivity perpendicular to the ladders is computed assuming incoherent tunneling giving a value close to experiment. [S0163-1829(98)51920-0]

$Sr_{14-x}Ca_xCu_{24}O_{41}$ (Refs. 1 and 2) is a material in which doped ladder (see Fig. 1) can be experimentally studied and compared to theoretical predictions of a Luther-Emery state with a spin gap, hole pairing, and superconductivity.[3–8] A spin gap of $\Delta \simeq 280$ K (for $x=9$) has been measured[9] and superconductivity under high pressure $P>3$ GPa has been found[9,10] in Ca-rich samples $x \simeq 11$ (Ca11), having ladder layers doped with 20% holes ($\delta \simeq 0.2$).[9,11,12] The transport properties are dominated by holes in the ladder planes. The normal state of the Ca11 shows a strong anisotropy between the dc resistivity along and across the ladder direction with $\rho_\perp/\rho_\parallel \simeq 30$ at $T=100$ K.[13] For lower temperature, both resistivities increase exponentially due to localization effects. For higher temperatures, $\rho_\parallel$ increases linearly in T while $\rho_\perp$ remains nearly constant, $\rho_\perp = 12$ mΩ cm. The mean free path along the ladder is larger than the lattice constant while across the ladders it is smaller than the interladder distance indicating incoherent transport in this direction.

Moreover, fits of the spin susceptibility have shown a large difference between the exchange coupling $J_\perp$ ($J_\parallel$) along the rungs (legs) of the ladder,[14,15] even if both involve similar 180° Cu-O-Cu superexchange processes. Analysis of neutron scattering data gives $J_\perp = 72$ meV and $J_\parallel = 130$ meV.[16] For these reasons a detailed examination of the electronic structure is desirable.

In this paper we present local-density approximation (LDA) calculations of the electronic structure, which give estimates of effective hopping matrix elements between states on different copper ions. The LDA studies are performed for $SrCu_2O_3$, a compound that possesses the same kind of Cu_2O_3 ladder planes as $Sr_{14-x}Ca_xCu_{24}O_{41}$ (see Fig. 1). Recently, Arai and Tsunetsugu[17] reported LDA calculations for $M_{14}Cu_{24}O_{41}$ (M = Sr or Ca), which give similar results.

The energy bands for $SrCu_2O_3$, computed with the tight-binding linear muffin-tin orbital, atomic sphere approximation (TB–LMTO ASA) (Ref. 18) are plotted in Fig. 1. The TB-LMTO ASA (Ref. 18) energy bands for $SrCu_2O_3$ are plotted in Fig. 2. The uppermost graph displays the bands on the path $\Gamma=(0,0,0)$, $Z'=(0,0,\pi/2c)$, $A'=(2\pi/a,0,\pi/2c)$, and $X=(2\pi/a,0,0)$. The two parallel bands near zero energy (Fermi energy of the half-filled band) are separated from the rest of the spectrum. They are due to hybridization through σ bonds of the $2p$ O orbitals and $3d_{x^2-z^2}$ Cu orbitals. These bands hybridize with nonbonding O bands near Γ. In the lower graph, the energy bands are shown up to the edge of the zone with $Z=(0,0,\pi/c)$ and $A=(2\pi/a,0,\pi/c)$. Due to destructive interference, the two d bands do not display dispersion on the path ZA.

The low energy physics can be described by an effective model containing only these two bands with similar shape near the Fermi energy. Such a model includes only one state per Cu with effective hopping matrix elements. These two bands are the bonding (b) and antibonding (a) rung bands of the effective ladder model.

Note that the parallel nature of the bands at $k_z=\pi/2c$ (path $Z'A'$) cannot be explained by effective interactions between nearest-neighbor (NN) Cu sites only. In such a model, the dispersion along the k_x direction is given by the interchain hopping matrix element between the second leg of one ladder and the first leg of the next ladder. Since the hopping matrix elements between two bonding (antibonding) states of the rung r of two neighboring ladders l and l'

$$b_{\sigma,l,r}(a_{\sigma,l,r}) = (1/\sqrt{2})[\phi_{\sigma,l,r,1} + (-)\phi_{\sigma,l,r,2}]$$

is given by

$$\langle b_{\sigma,l,r} H(t_{ll'}) b_{\sigma,l',r}\rangle = \langle \phi_{\sigma,l,r,2} H(t_{ll'}) \phi_{\sigma,l',r,1}\rangle,$$

$$\langle a_{\sigma,l,r} H(t_{ll'}) a_{\sigma,l',r}\rangle = -\langle \phi_{\sigma,l,r,2} H(t_{ll'}) \phi_{\sigma,l',r,1}\rangle, \quad (1)$$

where the last index of $\phi_{\sigma,l',r,1}$ labels the ladder leg. Therefore b and a states should have an opposite dispersion in the k_x direction. Thus, an effective atomic model must contain some longer range interladder hopping to account for their parallel nature.

Arai and Tsunetsugu introduced a simpler rung parametrization of the band structure fitting the b and a bands separately, allowing NN and next-nearest-neighbor hopping leading to the forms,[19]

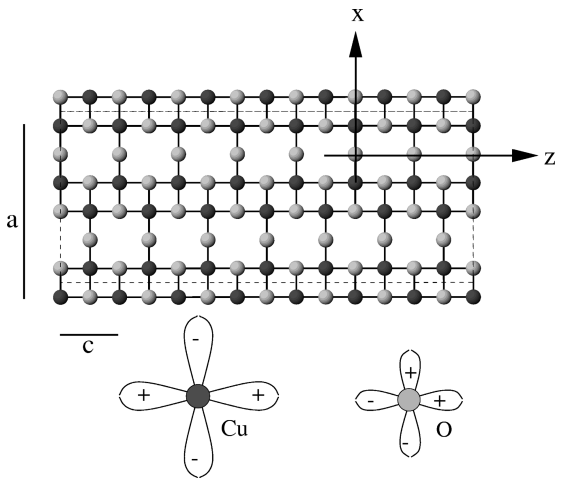

FIG. 1. The Cu_2O_3 ladder plane.

$$\epsilon(\mathbf{k}) = \epsilon_0 - 2h_{\parallel,1}\cos(k_z) - 2h_{\parallel,2}\cos(2k_z) - \left[4h_{\perp,1}\cos\left(\frac{1}{2}k_z\right) + 4h_{\perp,2}\cos\left(\frac{3}{2}k_z\right)\right]\cos(k_x). \tag{2}$$

The values they obtained for $Sr_{14}Cu_{24}O_{41}$ are in good qualitative agreement with ours for $SrCu_2O_3$ (see Table I). Note that the signs of the interladder hopping parameter $h_{\perp,1}$ does not change between an *a* band and *b* band contrary to the expectations from Eq. (1). All hopping parameters apart from $h_{\parallel,1}$ are higher order in the Cu-O (t_{pd}) and O-O overlaps t_{pp} and thus much smaller.

To gain more insight we introduce a single parametrization of both bands in terms of intersite hopping parameters shown in Fig. 3 The solution of this tight-binding model is

$$\epsilon_{\pm}(\mathbf{k}) = \epsilon_0 + \epsilon_{\parallel}(k_z) + \epsilon_{\perp,1}(k_z)\cos(k_x) \pm \sqrt{\epsilon_{\perp,3}(k_z)^2 + \epsilon_{\perp,4}(k_z)^2 + 2\epsilon_{\perp,3}(k_z)\epsilon_{\perp,4}(k_z)\cos(k_x)}, \tag{3}$$

where

$$\epsilon_{\parallel}(k_z) = -2t_{\parallel,1}\cos(k_z) - 2t_{\parallel,2}\cos(2k_z),$$

$$\epsilon_{\perp,1}(k_z) = -4t_{\perp,3}\cos\left(\frac{k_z}{2}\right) - 4t_{\perp,7}\cos\left(\frac{3k_z}{2}\right),$$

$$\epsilon_{\perp,3}(k_z) = t_{\perp,1} + 2t_{\perp,4}\cos(k_z) + 2t_{\perp,6}\cos(2k_z),$$

$$\epsilon_{\perp,4}(k_z) = 2t_{\perp,2}\cos\left(\frac{k_z}{2}\right) + 2t_{\perp,5}\cos\left(\frac{3k_z}{2}\right). \tag{4}$$

The parallel nature of the bands at $k_z = \pi/2$ is recovered if the term in the square root of Eq. (3) is independent of k_x. This is obtained if $\epsilon_{\perp,4}(\pi/2) \simeq 0$, leading to $t_{\perp,2}, t_{\perp,5} \simeq 0$ or to $t_{\perp,2} = t_{\perp,5}$. In these cases the dispersion at $k_z = \pi/2$ is due to the $\epsilon_{\perp,1}$ term being a function of $t_{\perp,3}$ and $t_{\perp,7}$. It clearly shows that an intersite model must contain at least the third-order hopping term $t_{\perp,3}$.

The coupled ladder system has a glide symmetry given by the product of a reflection through the *c* axis (see Fig. 3) and a translation of half a lattice constant along the ladder. When this operation is applied twice it is equivalent to a translation of one lattice constant along the ladder. This implies that the energy band at $k_x = 0$ and $k_x = \pi$ can be parametrized through one parameter. Actually $\epsilon_{\pm}(k_x = \pi, k_z) = \epsilon_{\pm}(k_x = 0, 2\pi - k_z)$ as can be directly checked from Eq. (3). This allows one to use a single function containing the information about all hopping parameters. This symmetry also implies the lack of dispersion in the k_x direction at $k_z = \pi$ as discussed above, as well as the square-root form containing intra- and inter-ladder hopping terms.

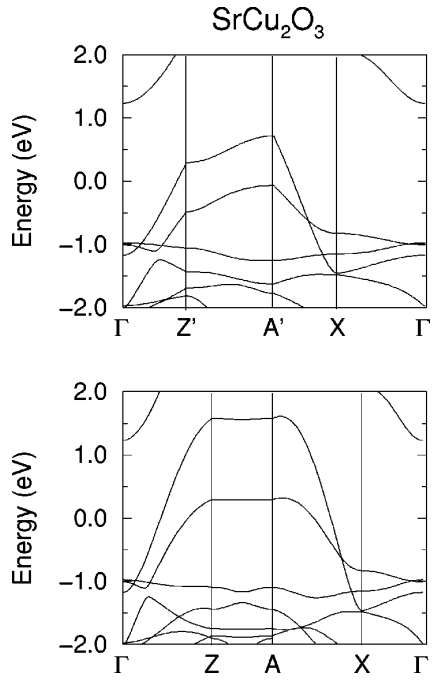

FIG. 2. LDA band calculations for $SrCu_2O_3$ on the path $\Gamma Z'A'X\Gamma$ (uppermost graph) and the path $\Gamma ZAX\Gamma$ (lower graph).

Introducing $\sigma = 1(-1)$ for $k_x = 0(\pi)$, Eq. (3) reduces to the simpler form

$$\epsilon_{\pm,\sigma}(k_z) = \epsilon_0 + \epsilon_{\parallel}(k_z) + \sigma\epsilon_{\perp,1}(k_z) \pm [\epsilon_{\perp,3}(k_z) + \sigma\epsilon_{\perp,4}(k_z)], \tag{5}$$

representing the four energy bands of the double-ladder system. Rewriting the bands from the rung form (2) to the intersite form (5) gives the values of Table II. They are consistent with each other and emphasize the dominance of the NN intraladder matrix elements $t_{\parallel}$ and $t_{\perp}$ with respect to the others. Moreover, they show surprisingly that these two parameters describing NN Cu-Cu processes differ from each other by $\sim 35\%$.

TABLE I. The hopping parameters in eV for $Sr_{14}Cu_{24}O_{41}$ (Ref. 17) and $SrCu_2O_3$ in the rung scheme.

	$Sr_{14}Cu_{24}O_{41}$		$SrCu_2O_3$	
	b band	*a* band	*b* band	*a* band
ϵ_0	−0.31	0.46	−0.44	0.35
$h_{\parallel,1}$	0.41	0.59	0.45	0.68
$h_{\parallel,2}$	0.08	0.07	0.08	0.07
$h_{\perp,1}$	0.07	0.03	0.07	0.03
$h_{\perp,2}$	0.00	−0.04	0.00	−0.04

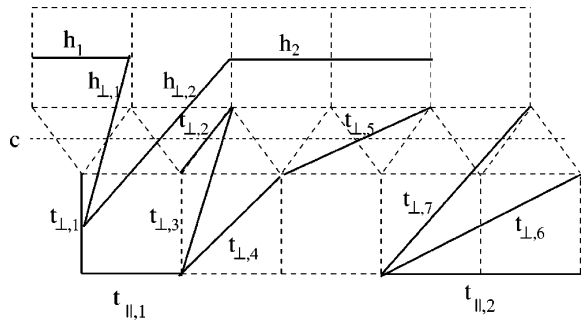

FIG. 3. Coupled ladders illustrating effective hoppings between Cu sites (t) or Cu-Cu rungs (h).

Recently, Andersen *et al.*[20,21] introduced a systematic downfolding scheme to obtain an effective single (or few) band model capable of reproducing the details of the LDA bands close to the Fermi level. Effective hopping parameters are calculated by performing the Fourier transform of the downfolded Hamiltonian $H(\mathbf{k})\rightarrow H(\mathbf{R})$, for $|\mathbf{R}|$ less than a cut-off radius R_0. This has the advantage among others that it allows the origin of the parameters in the effective single or few band model to be traced. We have applied this scheme to the LDA bands for $SrCu_2O_3$. The anisotropy $t_{\parallel,1}\neq t_{\perp,1}$ is best understood by starting with an effective model including the $3d_{x^2-z^2}$, $4s$ Cu orbitals and $2p_x$, $2p_z$ O orbitals (dsp model). The dominant parameters (>0.1 eV) for in-plane hopping are given in the first rows of Table III. Here $\mathbf{r}$ labels the O on the rung of one ladder while $\mathbf{l}$ labels either a Cu or an O on the *upper* leg of the ladder. Vectors $\mathbf{e}_x=(a/6,0,0)$ and $\mathbf{e}_z=(0,0,c/2)$ give the translation vector from one O(Cu) to the neighboring Cu(O) in the respective direction. The notation is such that $t_{d(\mathbf{l})p_x(+\mathbf{e}_x)}$ denotes the hopping between a $3d$ Cu orbital at $\mathbf{l}$ on the upper leg to the neighboring $2p_x$ O orbital at $\mathbf{l}+\mathbf{e}_x$. The on-site $t_{s(\mathbf{l})d(\mathbf{l})}$ hopping is nonzero as a consequence of the downfolding of all other bands in the absence of local fourfold symmetry.

The on-site energies of the rung oxygen $\epsilon(\mathbf{r})$ is slightly larger than that of the leg oxygen $\epsilon(\mathbf{l})$ due to the local environments. The distance between Cu and O is $r_l=1.98$ Å $\|\hat{z}$ and $r_r=1.92$ Å $\|\hat{x}$ implying a larger hopping along the x direction according to $t_{pd}\propto 1/r^4$ and explaining the anisotropy for the t_{pd}'s listed in the first row of Table III. Moreover, hopping processes involving s orbitals are large with non-negligible t_{sd} hoppings. The absence of local fourfold symmetry allows a direction dependent renormalization of the t_{pd} through the $4s$ Cu orbitals. In second order, the renormalization of $t_{d(\mathbf{l})p_x(-\mathbf{e}_x)}$ includes paths $d(\mathbf{l})$–$s(\mathbf{l})$–$p_x(\mathbf{l}-\mathbf{e}_x)$ and $d(\mathbf{l})$–$s(\mathbf{l}-2\mathbf{e}_x)$–$p_x(\mathbf{l}-\mathbf{e}_x)$($t^{(2)}_{d(\mathbf{l})p_x(-\mathbf{e}_x)}\simeq 0.69$ eV) whereas the renormalization of $t_{d(\mathbf{l})p_x(+\mathbf{e}_x)}$ involves only the path $d(\mathbf{l})$–$s(\mathbf{l})$–$p_x(\mathbf{l}+\mathbf{e}_x)$($t^{(2)}_{d(\mathbf{l})p_x(+\mathbf{e}_x)}\simeq -0.77$ eV). The renormalization in the leg direction $[t_{d(\mathbf{l})p_z(+\mathbf{e}_z)}]$ involves two paths with smaller d–s and s–p hoppings $[t^{(2)}_{d(\mathbf{l})p_z(+\mathbf{e}_z)}\simeq 0.77$ eV$]$.[22] Thus downfolding the s orbitals, giving the (dp) model, strongly renormalizes the t_{pd} such that $t_{d(\mathbf{l})p_x(-\mathbf{e}_x)}<t_{d(\mathbf{l})p_z(+\mathbf{e}_z)}$ as given in second row of Table III. Lastly, downfolding the p orbitals gives the effective (d) model. Results are given in the third column of Table II leading to $t_{\perp,1}<t_{\parallel,1}$. They are consistent with our previous results.

The exchange interaction J between spins are usually difficult to estimate *a priori*. In perturbation theory, J scales as t_{pd}^4 but given the large value of t_{pd} relative to $(\epsilon_p-\epsilon_d)$ the results are not reliable. Our analysis shows that the energy difference $(\epsilon_p-\epsilon_d)$ does not differ much between rung and legs but t_{pd} does. A ratio $J_{\perp,1}/J_{\parallel,1}<1$ is expected consistently with previous results[14–16]. This will disfavor the hole

TABLE II. The parameters in eV from direct fitting and downfolding of the LDA bands.

		$SrCu_2O_3$	
	$Sr_{14}Cu_{24}O_{41}$	Fit	Downfolding
ϵ_0	0.075	−0.045	−2.476
$t_{\parallel,1}$	0.500	0.565	0.537
$t_{\perp,1}$	0.385	0.395	0.351
$t_{\perp,2}$	0.040	0.040	0.018
$t_{\perp,3}$	0.050	0.050	0.050
$t_{\perp,4}$	−0.090	−0.115	−0.124
$t_{\perp,5}$	0.040	0.040	0.053
$t_{\parallel,2}$	0.075	0.075	0.106
$t_{\perp,6}$	0.005	0.005	0.012
$t_{\perp,7}$	−0.020	−0.020	−0.023

TABLE III. Hopping parameters in eV from the downfolding method. Notation is explained in the text.

	ϵ_d	$\epsilon_{p(\mathbf{r})}$	$\epsilon_{p(\mathbf{l})}$	$t_{d(\mathbf{l})p_z(+\mathbf{e}_z)}$	$t_{d(\mathbf{l})p_x(-\mathbf{e}_x)}$	$t_{d(\mathbf{l})p_x(+\mathbf{e}_x)}$	$t_{p_z(\mathbf{l})p_z(+\mathbf{e}_x+\mathbf{e}_z)}$
(dsp)	−3.82	−3.66	−4.00	0.74	0.85	−0.85	0.30
(dp)	−3.83	−4.59	−4.53	0.65	0.51	−0.63	0.22
	$t_{p_x(\mathbf{l})p_x(+\mathbf{e}_x+\mathbf{e}_z)}$	$t_{p_z(\mathbf{l})p_x(+\mathbf{e}_x+\mathbf{e}_z)}$		$t_{p_z(\mathbf{l})p_x(-\mathbf{e}_x+\mathbf{e}_z)}$	$t_{p_x(\mathbf{l})p_x(-\mathbf{e}_x+\mathbf{e}_z)}$	$t_{p_z(\mathbf{l})p_z(+2\mathbf{e}_z)}$	
(dsp)	0.30	0.01		−0.13	0.28	−0.42	
(dp)	0.62	0.62		−0.64	0.19	−0.05	
	$t_{p_x(\mathbf{l})p_x(+2\mathbf{e}_z)}$	$t_{p_x(\mathbf{r})p_x(+2\mathbf{e}_x)}$	ϵ_s	$t_{s(\mathbf{l})d(\mathbf{l})}$	$t_{s(\mathbf{l})d(+2\mathbf{e}_z)}$	$t_{s(\mathbf{l})s(+2\mathbf{e}_z)}$	
(dsp)	−0.17	−0.62	2.43	−0.24	−0.14	−0.32	
(dp)	−0.09	+0.31					
	$t_{s(\mathbf{l})d(-2\mathbf{e}_x)}$	$t_{s(\mathbf{l})s(-2\mathbf{e}_x)}$		$t_{s(\mathbf{l})p_z(+\mathbf{e}_z)}$	$t_{s(\mathbf{l})p_x(-\mathbf{e}_x)}$	$t_{s(\mathbf{l})p_x(+\mathbf{e}_x)}$	
(dsp)	0.20	−0.44		1.89	−2.28	2.07	

coupling and the singlet liquid state and may explain why holes are unbound for $T>100$ K, however, this point will not be discussed further.

In the following, two limiting estimates of the conductivity are investigated. First, the band-structure model limit is considered ignoring magnetic interactions although they must be important. In a metallic ground state, the conductivity reduces to an integral over the Fermi surface:

$$\sigma_{ij}=\frac{2e^2}{(2\pi)^2}\int d\mathbf{k}\tau[\epsilon(\mathbf{k})]v_i(\mathbf{k})v_j(\mathbf{k})\left(-\frac{\partial f}{\partial\epsilon}\right), \tag{6}$$

where τ is assumed constant at the Fermi energy. Considering an electron filling of $n=0.8$ the ratio between the conductivity perpendicular and parallel to the ladder can then be simply computed yielding very large values, i.e., $\sigma_\parallel/\sigma_\perp\simeq 75$, 90 and 104, for the parameter in Table II. Thus, roughly one has

$$\sigma_\parallel/\sigma_\perp\simeq 100. \tag{7}$$

This large anisotropy is a consequence of a warped Fermi surface with very small Fermi velocity perpendicular to the ladders.

Second, as discussed previously, the resistivity data perpendicular to the ladder indicates a mean free path smaller than the interladder spacing. Holes seem to be confined to ladders and to hop incoherently between them. A detail structural refinement of Ca11 (Ref. 23) shows a complex distortion pattern of the CuO_2 chains leading to substantial potential variations between rungs due to the proximity of apical O ions at $\sim 50\%$ of the rungs. An estimate of the interladder conductivity can be made by considering the limit where ladders form quasi-one-dimensional metallic systems weakly coupled to each other. The conductivity is thus a consequence of the interladder hopping term

$$H=\sum_{\mathbf{k}} T_k c^\dagger_{1,k}c_{2,k}+\text{H.c.}, \tag{8}$$

where $T_{\mathbf{k}}=\Sigma_i h_{\perp,i}(k)$. The conductance $\Sigma_\perp$ is given by

$$\Sigma_\perp=4\pi\frac{e^2}{\hbar}\mathcal{N}(\epsilon_F)^2|T(k_F)|^2, \tag{9}$$

with $\mathcal{N}(\epsilon_F)$ denoting the density of state at E_F in the quasi-one-dimensional metallic system. Results for the different parameter sets are the conductivities $\sigma_\perp\simeq 0.1$, 0.09, and 0.074, respectively. They are thus all close the value of

$$\sigma_\perp\simeq 0.08\ \ (\text{m}\Omega\ \text{cm})^{-1}, \tag{10}$$

which corresponds well with the experimental result at $T\geqslant 100$ K.

In this paper, estimates of the hopping matrix elements based on LDA calculations gave three main results. First, the effective intraladder hopping between NN are not the same, $t_\parallel\neq t_\perp$. This was explained as the consequence of anisotropic t_{pd} in the (pd) model due to effective hopping through paths involving Cu $4s$ states. Second, interladder hopping is much smaller than intraladder and longer range hopping must be included. Third, estimates of the conductivity in the model where holes are unbound and confined into the ladder give good agreement with the experiment at temperatures $T\geqslant 100$ K.

One of us (T. M.) thanks the ''Fond National Suisse'' for financial support. We would like to thank O. K. Andersen and M. Troyer for useful and fruitful discussions.

[1] E. M. McCarron, M. A. Subramanian, J. C. Calabrese, and R. L. Harlow, Mater. Res. Bull. **23**, 1355 (1988).
[2] T. Siegrist, L. F. Schneemeyer, S. A. Sunshine, and J. V. Waszczak, Mater. Res. Bull. **23**, 1429 (1988).
[3] E. Dagotto, J. Riera, and D. Scalapino, Phys. Rev. B **45**, 5744 (1992).
[4] T. M. Rice, S. Gopalan, and M. Sigrist, Europhys. Lett. **23**, 445 (1993).
[5] S. Gopalan, T. M. Rice, and M. Sigrist, Phys. Rev. B **49**, 8901 (1994).
[6] H. Tsunetsugu, M. Troyer, and T. M. Rice, Phys. Rev. B **51**, 16 456 (1995).
[7] M. Toyer, H. Tsunetsugu, and T. M. Rice, Phys. Rev. B **53**, 251 (1996).
[8] C. A. Hayward and D. Poilblanc, Phys. Rev. B **53**, 11 721 (1996).
[9] K. Magishi, S. Matsumoto, Y. Kitaoka, K. Ishida, K. Asayama, M. Uehara, T. Nagata, and J. Akimitsu, Phys. Rev. B (to be published 1 May 1998).
[10] M. Uehara, T. Nagata, J. Akimitsu, H. Takahashi, N. Môri, and K. Kinoshita, J. Phys. Jpn. **65**, 2764 (1996).
[11] T. Osafune, N. Motoyama, H. Eisaki, and S. Uchida, Phys. Rev. Lett. **78**, 1980 (1997).
[12] Y. Mizuno, T. Tohyama, and S. Maekawa, J. Phys. Soc. Jpn. **4**, 937 (1997).
[13] N. Motoyama, T. Osafune, T. Kakeshita, H. Eisaki, and S. Uchida, Phys. Rev. B **55**, 3386 (1997).
[14] D. C. Johnston, Phys. Rev. B **54**, 13 009 (1996); D. C. Johnston, M. Troyer, S. Miyahara, D. Lidski, K. Ueda, M. Azuma, Z. Hiroi, M. Takano, M. Isobe and Y. Ueda, Bull. Am. Phys. Soc. **43**, 705 (1998).
[15] M. Troyer (private communication).
[16] R. S. Eccleston M. Uehara, J. Akimitsu, H. Eisaki, M. Motoyama, and S. Uchida, cond-mat/9711053.
[17] M. Arai and H. Tsunetsugu, Phys. Rev. B **56**, R4305 (1997).
[18] O. K. Andersen and O. Jepsen, Phys. Rev. Lett. **53**, 2571 (1984).
[19] We use the notation $k_x a/2\rightarrow k_x$ and $k_z c\rightarrow k_z$.
[20] O. K. Andersen, O. Jepsen, and G. Krier, in *Lectures on Methods of Electronic Structure Calculations,* edited by V. Kumar, O. K. Andersen, and A. Mookerjee (World Scientific, Singapore, 1994), pp. 63–124; T. Saha-Dasgupta, O. K. Andersen, C. Arcangeli, R. W. Tank, G. Krier, and O. Jepsen (unpublished).
[21] O. K. Andersen, O. Jepsen, A. I. Liechtenstein, and I. I. Mazin, Phys. Rev. B **49**, 4145 (1994).
[22] In this order the renormalization leads to an increase due to the dominant $d(\mathbf{l})-s(\mathbf{l})-p_z(\mathbf{l}+\mathbf{e}_z)$ path.
[23] T. Ohta, F. Izumi, M. Onoda, M. Isobe, E. Takayama-Muromachi, and W. Hewat, J. Phys. Soc. Jpn. **66**, 3107 (1997); M. Isobe, T. Ohta, M. Onada, F. Izumi, S. Nakano, J. Q. Li, Y. Matsui, and E. Takayama-Muromachi, Phys. Rev. B **57**, 613 (1998).